Current Biology 23, 924–929, May 20, 2013 ©2013 Elsevier Ltd All rights reserved http://dx.doi.org/10.1016/j.cub.2013.04.025

Report

An Iron-Rich Organelle in the Cuticular Plate of Avian Hair Cells

Mattias Lauwers,[1,5] Paul Pichler,[1,5] Nathaniel Bernard Edelman,[1] Guenter Paul Resch,[2] Lyubov Ushakova,[1] Marion Claudia Salzer,[1] Dominik Heyers,[3] Martin Saunders,[4] Jeremy Shaw,[4] and David Anthony Keays[1,*]

[1]Institute of Molecular Pathology, Dr. Bohr-Gasse 7, 1030 Vienna, Austria

[2]Campus Science Support Facilities, Dr. Bohr-Gasse 3, 1030 Vienna, Austria

[3]Animal Navigation, Institut für Biologie und Umweltwissenschaften, University of Oldenburg, 26111 Oldenburg, Germany

[4]Centre for Microscopy, Characterisation and Analysis, The University of Western Australia, Crawley, WA 6009, Australia

Summary

Hair cells reside in specialized epithelia in the inner ear of vertebrates, mediating the detection of sound, motion, and gravity. The transduction of these stimuli into a neuronal impulse requires the deflection of stereocilia, which are stabilized by the actin-rich cuticular plate. Recent electrophysiological studies have implicated the vestibular system in pigeon magnetosensation [1]. Here we report the discovery of a single iron-rich organelle that resides in the cuticular plate of cochlear and vestibular hair cells in the pigeon. Transmission electron microscopy, coupled with elemental analysis, has shown that this structure is composed of ferritin-like granules, is approximately 300–600 nm in diameter, is spherical, and in some instances is membrane-bound and/or organized in a paracrystalline array. This organelle is found in hair cells in a wide variety of avian species, but not in rodents or in humans. This structure may function as (1) a store of excess iron, (2) a stabilizer of stereocilia, or (3) a mediator of magnetic detection. Given the specific subcellular location, elemental composition, and evolutionary conservation, we propose that this structure is an integral component of the sensory apparatus in birds.

Results

In vertebrates, the detection of sound, motion, and gravity is mediated by a remarkable set of sensory receptors known as hair cells. The transduction of these stimuli into a neuronal impulse involves the deflection of hair cell stereocilia, which applies a tensile force to specialized structures known as tip links, opening cation channels [2, 3]. The stereocilia are stabilized by the actin-rich cuticular plate, which facilitates the return of cilia to their resting position following the application of a mechanical force. The cuticular plate is, in turn, anchored in place by the striated organelle, which is a cytoskeletal lattice located basally [4, 5]. These cellular structures are responsible for the sensitivity and functional properties of hair cells.

In birds, hair cells are found in an ensemble of sensory structures in the inner ear that include the utricle, the saccule, the lagena, and the basilar papilla (Figure 1A). The basilar papilla, which is the avian equivalent of the organ of Corti, is primarily responsible for the detection of sound, whereas the lagena, utricle, and saccule are believed to be involved in the detection of linear acceleration (Figure 1A) [10]. Recently, work by Dickman and colleagues has implicated the inner ear in magnetoreception in pigeons [1, 11]. Employing c-Fos as a marker for neuronal activation and single-cell electrophysiology, they identified a population of neurons in the vestibular nuclei that are sensitive to the intensity and polarity of magnetic stimuli. They showed that magnetically induced c-Fos activation in the posterior medial and descending vestibular nuclei was dependent on an intact cochlear duct, which encompasses both the basilar papilla and the lagena [11]. This result raises the prospect that sensory cells in the inner ear, perhaps hair cells, act as the primary magnetosensors. Because it is conceivable that these cells use the iron oxide magnetite (Fe_3O_4) to transduce local magnetic information into a neuronal impulse [12], in this study we employ histological and ultrastructural methods to identify iron-rich cells in the inner ear of pigeons.

The Discovery of Iron-Rich Sensory Hair Cells

To detect iron-rich cells in the vestibular and auditory system of pigeons, we employed the Prussian blue (PB) chemical stain, which labels ferric iron (Fe^{3+}) (n = 39 birds). Examination of histological sections with light microscopy revealed the presence of a PB-positive structure in a proportion of hair cells in the basilar papilla, lagena, saccule, and utricle (Figures 1E–1H). In almost all instances, we observed only one PB-positive structure per cell, which was always apically located beneath the stereocilia (Figure 1D). In the basilar papilla, the PB-positive structure was found in both tall and short hair cells. Staining with the hair cell marker otoferlin confirmed that the iron-rich structure was restricted to sensory cells and was not present in support or hyaline cells (see Figures S1A–S1C available online). Analysis of dissociated hair cells in solution revealed that these subcellular structures can be identified by transmitted light microscopy (Figures 1J–1M). We exploited this to determine whether they are found in flask-shaped type I hair cells and/or column-shaped type II hair cells in the lagena. We adopted the method of Ricci and colleagues of plotting the ratio of the neck width to cuticular plate width (NPR), versus the ratio of the neck width to the body width (NBR) (Figure 1I) (n = 6 birds, n = 43 hair cells containing iron-rich structures, n = 43 hair cells without an iron-rich structure) [8, 9]. This analysis revealed that iron-rich structures are present in both type I and type II hair cells in the lagena (Figure 1I–1M).

Quantitation and Distribution of Iron-Rich Hair Cells

To gain further insight into the role of this structure, we undertook a quantitative analysis of the number and distribution of PB-positive hair cells in our histological sections, with a focus on the cochlear duct. Following the assignment of five anatomical landmarks along the pigeon cochlear duct and the creation of an anatomical standard (Figure 2A), we

[5]These authors contributed equally to this work

*Correspondence: keays@imp.ac.at

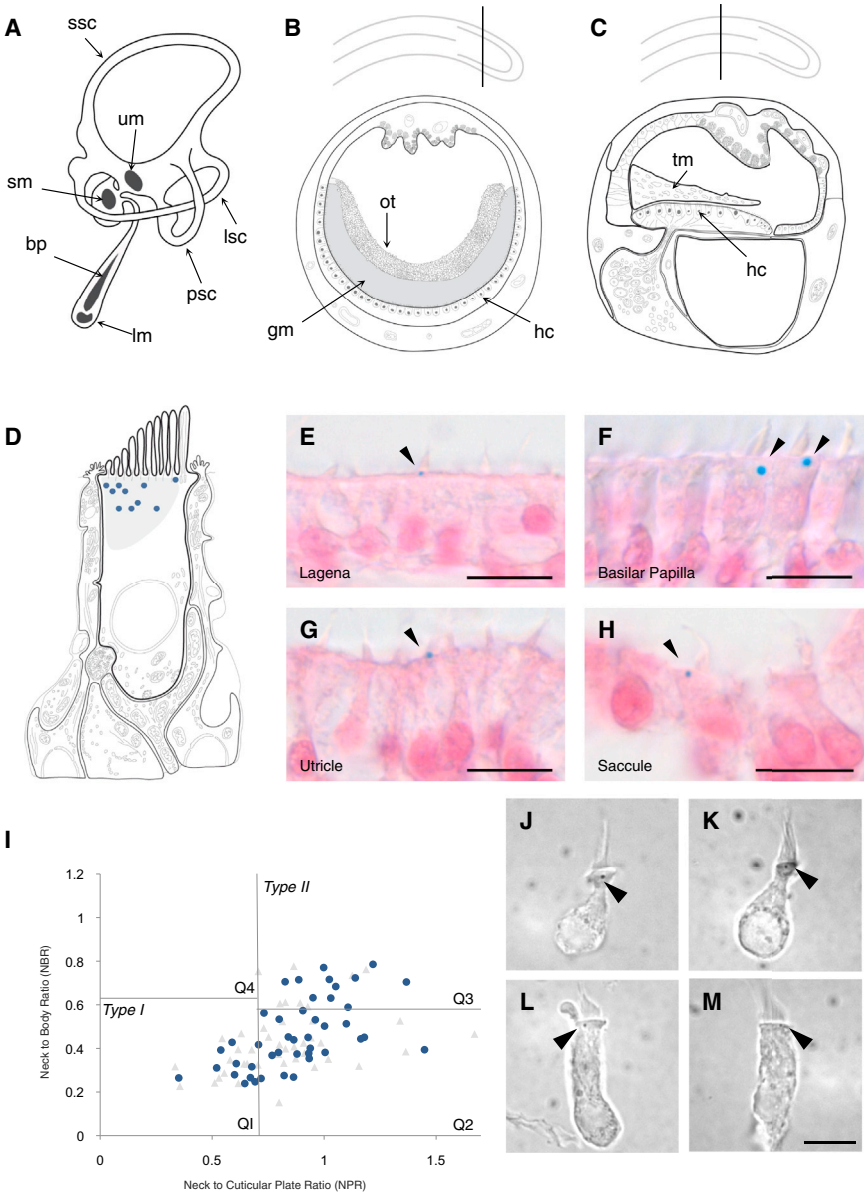

Figure 1. The Discovery of an Iron-Rich Structure in Pigeon Hair Cells

(A) Diagram of the pigeon inner ear, highlighting the superior semicircular canal (ssc), the lateral semicircular canal (lsc), the posterior semicircular canal (psc), the utricular macula (um), the saccular macula (sm), the basilar papilla (bp), and the lagena macula (lm). Diagram is adapted from [6].

(B) Diagram of a cross-section through the lagena macula, highlighting the calcium carbonate otoliths (ot) that are associated with a gelatinous membrane (gm) overlaying the hair cells (hc).

(C) Diagram of a cross-section through the basilar papilla, highlighting the tectorial membrane (tm) and the hair cells (hc). For (B) and (C), the position of the cross-section is shown above on a lateral view of the cochlear duct with a line.

(D) Diagram showing the location of the iron-rich structure from ten different tall hair cells (blue dots). In all instances, the iron-rich structure was found in the cuticular plate beneath the stereocilia. Diagrams in (B)–(D) are adapted from [7].

(E–H) Images of sections stained with Prussian blue and nuclear fast red (NFR) from the pigeon lagena (E), basilar papilla (F), utricle (G), and saccule (H). Arrowheads highlight the Prussian blue-positive structure in each hair cell.

(I) Morphometric analysis of dissociated hair cells. The neck to cuticular plate ratio (NPR) is plotted against the neck to body ratio (NBR) to ascertain whether a cell is a type I or type II hair cell. Cells without the iron-rich structure are plotted as gray triangles, and cells containing iron-rich structures are plotted as blue dots. Quadrant boundaries are those adopted by Ricci and colleagues, where quadrant 1 is enriched for flask-shaped type I hair cells and quadrant 3 is enriched for column-shaped type II hair cells [8, 9].

(J–M) Representative type I hair cells from quadrant 1 (J and K) and representative type II hair cells from quadrant 3 (L and M). Arrowheads highlight iron-rich structures.

All scale bars represent 10 μm.

manually counted PB-positive hair cells, mapping their distribution along the basilar papilla and the lagena (n = 6) (Figures S2A–S2F; Table S1). In the basilar papilla, we found that 28.0% of hair cells were PB-positive (n = 6 birds, n = 15,876 cells) and that these cells were represented in greater numbers in the medial to distal regions of this spatula-shaped structure (Figure 2B). In the lagena, we found that only 1.8% of hair cells were PB-positive (n = 6 birds, n = 20,858 cells), and these cells were found in both the striolar and extrastriolar regions of the epithelia (Figures S2G–S2I). We found that 2.9% of hair cells were PB-positive in the saccule (n = 6 birds, n = 4,400 cells) and 5.7% were PB-positive in the utricle (n = 5 birds, n = 13,640 cells). Statistical analysis revealed that there was a significant difference in the percentage of PB-positive cells in the basilar papilla when compared with the lagena ($p < 0.0001$), the utricle ($p < 0.0001$), and the saccule ($p < 0.0001$). There were no significant differences observed when comparing the lagena and the saccule ($p > 0.5$) or the saccule and the utricle ($p > 0.1$), but there were when comparing the lagena and the utricle ($p < 0.05$). Comparison of the percentage of PB-positive cells from left and right cochlear ducts revealed no statistically significant differences, indicating that iron-rich cells are not lateralized in pigeons (lagena: $p > 0.5$; basilar papilla: $p > 0.1$). We then undertook a quantitative assessment of the number of PB-positive structures present in a hair cell, given that the hair cell contains at least one such structure. This revealed that 99.71% of PB-positive hair cells in the lagena (n = 14 birds, n = 879 cells), 97.86% of PB-positive hair cells in the basilar papilla (n = 14 birds, n = 9,128 cells), 99.67% of PB-positive hair cells in the utricle (n = 6 birds, n = 811 cells), and 98.69% of PB-positive hair cells in the saccule (n = 5 birds, n = 104 cells) had a single iron-rich structure present (Figure 2D). Our total hair cell counts were consistent with previous studies performed in pigeons [13].

The Subcellular Architecture of Iron-Rich Hair Cells

To visualize the subcellular architecture of PB-positive hair cells, we employed correlative light and electron microscopy (CLEM) and electron tomography [14]. This revealed the presence of an electron-dense spherical structure with an average

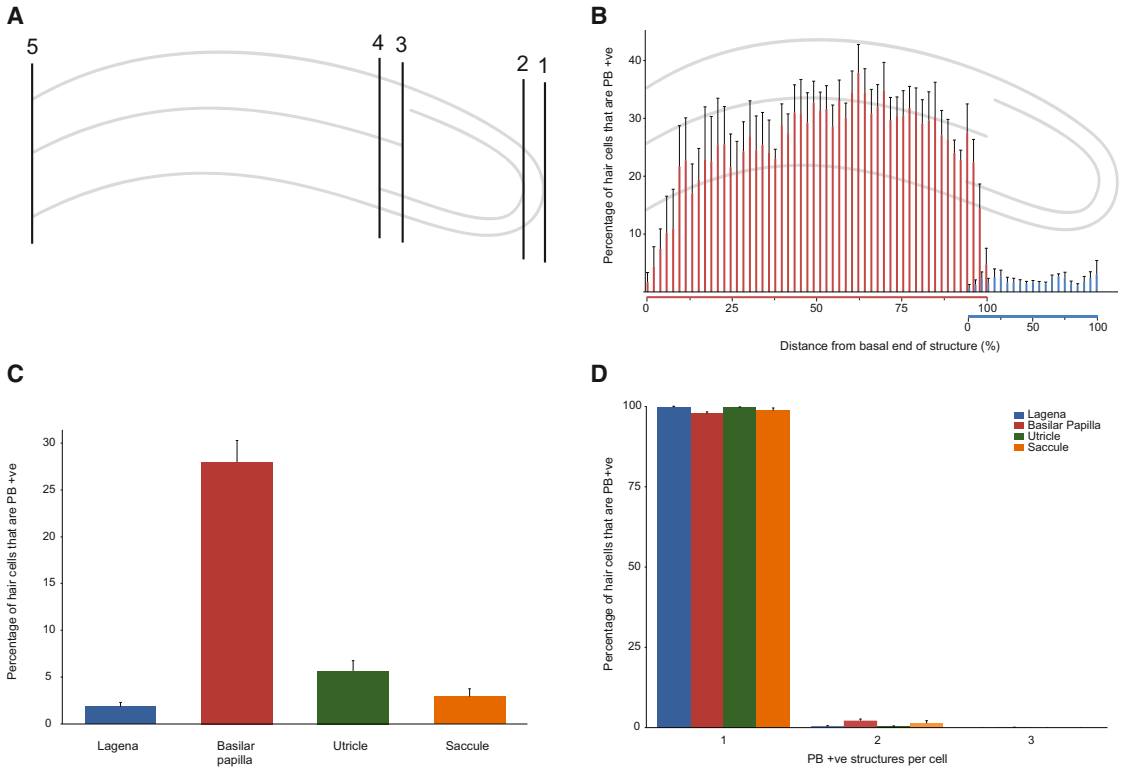

Figure 2. Quantitation and Distribution of PB-Positive Hair Cells in Pigeons

(A) Cochlear duct schematic showing the five landmarks employed to map the distribution of PB-positive hair cells: (1) the end of the cochlear duct, (2) the beginning of the lagena, (3) the beginning of the basilar papilla, (4) the end of the lagena, and (5) the end of the basilar papilla.

(B) Graph showing the percent of hair cells that are PB-positive (y axis) along the length of the basilar papilla (shown in red) and the lagena macula (shown in blue) from their basal ends (n = 6 birds).

(C) Graph showing the percentage of hair cells that contain a PB-positive structure in the lagena (1.8%, n = 6 birds, n = 20,858 cells), basilar papilla (28.0%, n = 6 birds, n = 15,876 cells), utricle (5.6%, n = 5 birds, n = 13,640 cells), and saccule (2.9%, n = 6 birds, n = 4,400 cells).

(D) Graph showing the percentage of PB-positive cells that contain one, two, or three iron-rich structures. A single iron-rich structure is found in 99.71% of cells in the lagena (n = 14 birds, n = 879 cells), 97.86% of cells in the basilar papilla (n = 14 birds, n = 9,128 cells), 99.67% of cells in the utricle (n = 6 birds, n = 811 cells), and 98.69% of cells in the saccule (n = 5 birds, n = 104 cells).

The error bars in (B)–(D) show the SEM.

diameter of 545 ± 31.4 nm (n = 18) in cochlear hair cells and 365 ± 27.2 nm (n = 16) in vestibular hair cells (Figures 3A–3F). In some but not all instances, this subcellular structure was membrane bound (22%, n = 44) (Figures 3A, 3C, and 3E; Movie S1), decorated with smaller vesicles (25%, n = 44) (Figure 3B; Movie S2), or appeared to be in the process of flux (7%, n = 44) (Figure S3E). Imaging by transmission electron microscopy (TEM) showed that each iron-rich subcellular structure is composed of hundreds of ferritin-like granules that have a diameter of 6.75 ± 0.06 nm in the basilar papilla (n = 319 particles, n = 3 birds) and 6.48 ± 0.06 nm in vestibular hair cells (n = 268 particles, n = 4 birds) (Figure 3G) [15]. On a number of occasions, these particles were ordered in striking paracrystalline arrays (16%, n = 44) (Figures 3E, 3F, and 3H; Movie S3). Consistent with our histological studies, energy-filtered transmission electron microscopy (EFTEM) and electron energy loss spectroscopy (EELS) confirmed that each structure is iron rich (n = 3) (Figures S3A–S3C). Selected area electron diffraction analysis (SAED) indicated that the dominant iron species within each organelle is ferrihydrite (Figure S3D).

Iron-Rich Hair Cells in Avian Species

Next, we asked whether this iron-rich subcellular structure is unique to pigeons or whether it is also found in other avian species. To address this, we dissected out the inner ear and performed the aforementioned histological characterization on birds from a variety of different orders including Passeriformes, Psittaciformes, Anseriformes, Galliformes, and Struthioniformes. We analyzed zebra finches (*Taeniopygia guttata*, n = 3), ducks (*Anas platyrhynchos domesticus*, n = 2), chickens (*Gallus gallus domesticus*, n = 3), ostriches (*Struthio camelus*, n = 2), and budgerigars (*Melopsittacus undulates*, n = 3). In all species analyzed, we observed apically located PB-positive structures in either the basilar papilla or the vestibular epithelia (Figure 4). We do not, however, find PB-positive structures in rats (*Rattus rattus*, n = 3), mice (*Mus musculus*, n = 5), guinea pigs *(Cavia porcellus*, n = 3), humans (*Homo sapiens*, n = 2), zebrafish (*Danio rerio*, n = 4), or rainbow trout (*Oncorhynchus mykiss*, n = 4) (Figure S4). The result shows that this iron-rich structure is conserved in Aves.

Discussion

We report the discovery of an iron-rich structure in avian hair cells that has a number of striking features: (1) it is located apically in the cuticular plate, (2) there is almost always only one per cell, (3) it is spherical in shape, (4) it is composed of ferritin-like granules, and (5) available data indicate that these

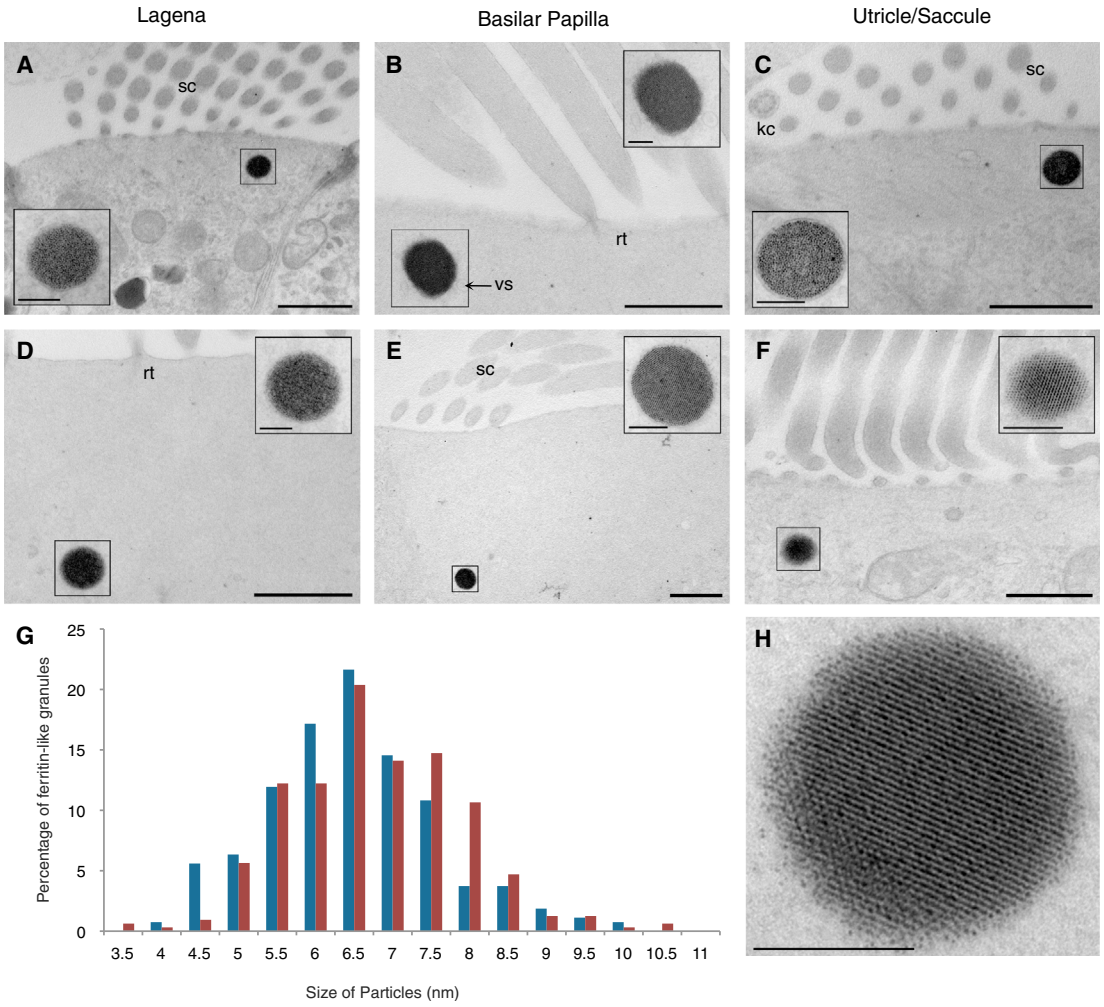

Figure 3. Subcellular Architecture of PB-Positive Hair Cells in Pigeons

(A–F) TEM images of iron-rich hair cells from the lagena (A and D), basilar papilla (B and E), utricle (C), and saccule (F). Each cell contains an electron-dense spherical structure that is located in the cuticular plate and is composed of ferritin-like granules that are on average 6–7 nm in size. In some instances, these granules are organized in a paracrystalline array (E, F, and H). This organelle is surrounded by a membrane in panels (A), (C), and (E) and is decorated with vesicles in (B). The stereocilia (sc), the rootlets of the stereocilia (rt), the kinocilium (kc), and vesicles (vs) are labeled accordingly.

(G) Size distribution of ferritin-like granules that make up iron-rich organelles in the basilar papilla (red bars) and vestibular hair cells (blue bars).

(H) Shows a high-magnification image of an organelle consisting of ferritin-like granules that are ordered in parallel lines.

Scale bars represent 1 μm in (A)–(F) main images and 200 nm in (A)–(F) insets and in (H).

granules consist of ferrihydrite. In some but not all instances, these structures are membrane bound and are composed of particles that are arranged in a paracrystalline array. The structures we observe are similar in appearance to siderosomes, which are iron-storage organelles found in macrophages and ferruginous micelles found in erythroblasts [14, 16–18], with the notable exception of their subcellular location and frequency. To reflect this difference, we refer to the structures identified as "cuticulosomes." It is known that siderosomes are derived from lysosome-like compartments that accumulate iron within a membrane-bound body [15]. We do not know whether cuticulosomes are formed in the vicinity of the endoplasmic reticulum and are transported into the cuticular plate or, alternatively, form within it. Our electron micrograph data hint at the latter, given that we observed a number of organelles, which appear to be immature, that already reside within this actin-rich meshwork.

What is the function of cuticulosomes in hair cells? We consider the following to be possibilities: (1) a store of excess iron, (2) a stabilizer of stereocilia, or (3) a mediator of magnetoreception. Although it is possible that this structure is a simple iron store (i.e., a siderosome), this would seem unlikely. There is no evidence that sensory neurons play a role in iron homeostasis, and it is not clear why a role in iron storage would necessitate the conspicuous positioning of a single organelle in the cuticular plate. Moreover, the absence of this organelle in rodents, humans, and the majority of avian hair cells indicates that the presence of the organelle is not required for cell viability. An alternative explanation for the presence of an iron sphere in the cuticular plate is that it reinforces stereocilia by acting as an intracellular pendulum, facilitating their return to the resting position. This would be mediated by the increased density of the iron in comparison to its actin-rich surroundings, but it would necessitate a cytoskeletal connection [4]. It is conceivable that this stabilization might alter the mechanically induced transductive properties of stereocilia, enhancing the detection of low-frequency sound, including infrasound (f < 20 Hz, λ > 17.2 m). This idea is supported by

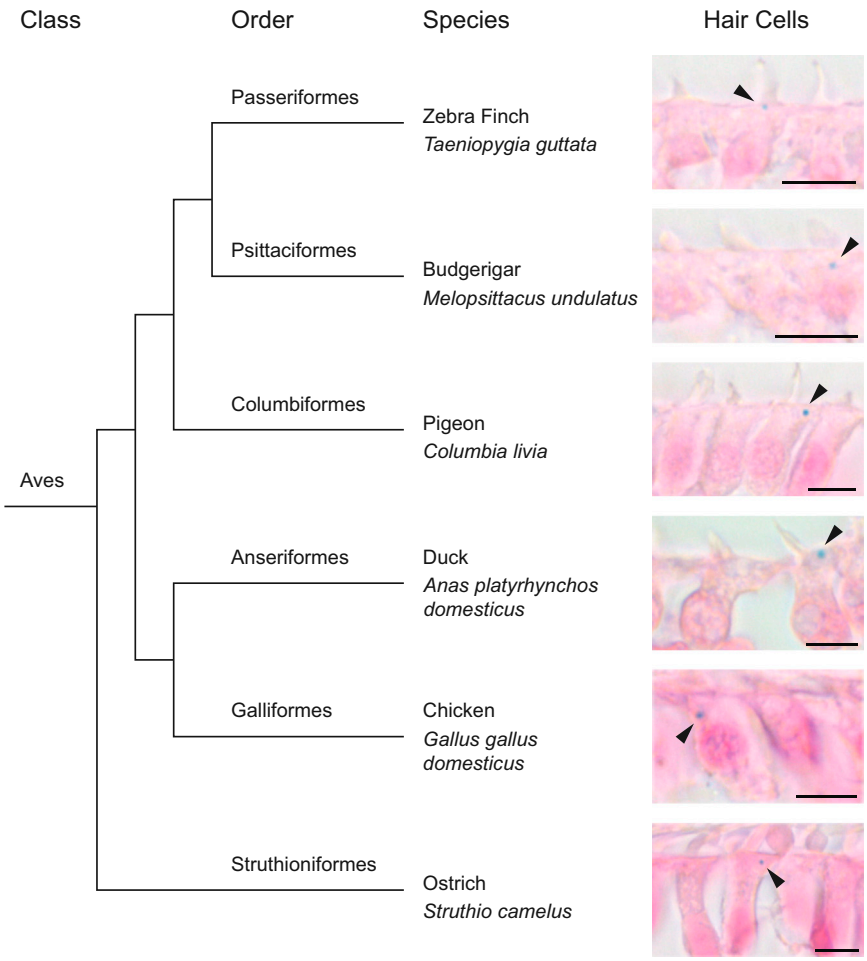

Figure 4. PB-Positive Hair Cells in Avian Species

Phylogenic tree of avian species that includes the Passeriformes, Psittaciformes, Columbiformes, Anseriformes, Galliformes, and Struthioniformes. Panels on the right show sections stained with NFR and PB. Images shown are cochlear hair cells, with the exception of the zebra finch (lagenar hair cells). We observed PB-positive structures (arrowheads) in all avian species analyzed in either cochlear or vestibular hair cells. Each PB-positive structure was located apically beneath the stereocilia. The scale bar represents 5 μm.

our observation that iron-rich organelles are enriched in the medial to distal regions of the basilar papilla (which are tuned to sounds with longer wavelengths); however, it fails to account for their presence in vestibular hair cells.

Might cuticulosomes mediate magnetoreception? This is a tempting proposition, particularly given that we have not identified any other iron-rich cells in the inner ear of pigeons; however, it should be viewed critically. Although it has been shown that the iron within ferritin cores includes magnetite [19, 20], our elemental analysis reveals that the dominant species of iron within the organelle is ferrihydrite. This composition is inconsistent with current models of a torque-based magnetoreceptor constructed of single-domain magnetite [21]. Studies in yeast and cell culture systems have artificially conferred magnetic properties on eukaryotic cells by overexpressing ferritin; however, these experiments have relied on the application of large external fields that are many times stronger than the Earth's [22, 23]. In addition, it is difficult to reconcile the electrophysiological studies conducted by Dickman and colleagues [1, 11] with the abundance of PB-positive hair cells in the basilar papilla in comparison to the few observed in the vestibular epithelia. It will be important to establish whether afferents from the basilar papilla innervate regions of the vestibular nucleus in pigeons, and whether calcium influx is induced by the application of a magnetic stimulus in iron-rich cells. Functional interrogation of this organelle will be a challenging task, particularly given the limited transgenic and molecular technologies available in birds. This goal is nonetheless worthy of pursuit, given that the specific subcellular location, elemental composition, and conservation indicate that it is an integral component of the avian sensory apparatus.

Supplemental Information

Supplemental Information includes four figures, one table, Supplemental Experimental Procedures, and three movies and can be found with this article online at http://dx.doi.org/10.1016/j.cub.2013.04.025.

Acknowledgments

We wish to thank the bio-optics, histology, electron microscopy, and graphics departments at the Institute of Molecular Pathology for their help. We are similarly indebted to the Centre for Microscopy, Characterisation and Analysis and the Australian Microscopy and Microanalysis Research Facility at The University of Western Australia, a facility funded by the University, State, and Commonwealth Governments. D.H. is supported by the German Research Foundation (DFG, HE 6221/1-1). We thank the Max F. Perutz Laboratories fish facility for providing the zebrafish used in the study. Finally, we wish to express our sincere thanks to Boehringer Ingelheim, which funds research at the Institute of Molecular Pathology. D.A.K. is an EMBO young investigator. Experiments were performed in accordance with the relevant guidelines and regulations (Magistrat 60, MA60-001603/2010/002).

Received: January 28, 2013
Revised: March 18, 2013
Accepted: April 9, 2013
Published: April 25, 2013

References

1. Wu, L.Q., and Dickman, J.D. (2012). Neural correlates of a magnetic sense. Science *336*, 1054–1057.
2. Hudspeth, A.J., and Jacobs, R. (1979). Stereocilia mediate transduction in vertebrate hair cells (auditory system/cilium/vestibular system). Proc. Natl. Acad. Sci. USA *76*, 1506–1509.
3. Pickles, J.O., Comis, S.D., and Osborne, M.P. (1984). Cross-links between stereocilia in the guinea pig organ of Corti, and their possible relation to sensory transduction. Hear. Res. *15*, 103–112.
4. Vranceanu, F., Perkins, G.A., Terada, M., Chidavaenzi, R.L., Ellisman, M.H., and Lysakowski, A. (2012). Striated organelle, a cytoskeletal structure positioned to modulate hair-cell transduction. Proc. Natl. Acad. Sci. USA *109*, 4473–4478.
5. Friedmann, I., Cawthorne, T., and Bird, E.S. (1965). Broad-banded striated bodies in the sensory epithelium of the human macula and in neurinoma. Nature *207*, 171–174.
6. Hofman, R., Segenhout, J.M., and Wit, H.P. (2009). A Bast-like valve in the pigeon? Eur. Arch. Otorhinolaryngol. *266*, 1397–1401.
7. Takasaka, T., and Smith, C.A. (1971). The structure and innervation of the pigeon's basilar papilla. J. Ultrastruct. Res. *35*, 20–65.
8. Ricci, A.J., Cochran, S.L., Rennie, K.J., and Correia, M.J. (1997). Vestibular type I and type II hair cells. 2: Morphometric comparisons of dissociated pigeon hair cells. J. Vestib. Res. *7*, 407–420.
9. Ricci, A.J., Rennie, K.J., Cochran, S.L., Kevetter, G.A., and Correia, M.J. (1997). Vestibular type I and type II hair cells. 1: Morphometric identification in the pigeon and gerbil. J. Vestib. Res. *7*, 393–406.
10. Manley, G.A. (1990). Peripheral Hearing Mechanisms in Reptiles and Birds (Heidelberg, Germany: Springer-Verlag).
11. Wu, L.Q., and Dickman, J.D. (2011). Magnetoreception in an avian brain in part mediated by inner ear lagena. Curr. Biol. *21*, 418–423.
12. Kirschvink, J.L., Walker, M.M., and Diebel, C.E. (2001). Magnetite-based magnetoreception. Curr. Opin. Neurobiol. *11*, 462–467.
13. Gleich, O., and Manley, G.A. (1988). Quantitative morphological analysis of the sensory epithelium of the starling and pigeon basilar papilla. Hear. Res. *34*, 69–85.
14. Treiber, C.D., Salzer, M.C., Riegler, J., Edelman, N., Sugar, C., Breuss, M., Pichler, P., Cadiou, H., Saunders, M., Lythgoe, M., et al. (2012). Clusters of iron-rich cells in the upper beak of pigeons are macrophages not magnetosensitive neurons. Nature *484*, 367–370.
15. Iancu, T.C. (1992). The ultrastructural spectrum of lysosomal storage diseases. Ultrastruct. Pathol. *16*, 231–244.
16. Iancu, T.C. (1992). Ferritin and hemosiderin in pathological tissues. Electron Microsc. Rev. *5*, 209–229.
17. Richter, G.W. (1957). A study of hemosiderosis with the aid of electron microscopy; with observations on the relationship between hemosiderin and ferritin. J. Exp. Med. *106*, 203–218.
18. Bessis, M.C., and Breton-Gorius, J. (1959). Ferrtin and ferruginous micelles in normal erythroblasts and hypochromic hypersideremic anemias. Blood *14*, 423–432.
19. Gálvez, N., Fernández, B., Sánchez, P., Cuesta, R., Ceolín, M., Clemente-León, M., Trasobares, S., López-Haro, M., Calvino, J.J., Stéphan, O., and Domínguez-Vera, J.M. (2008). Comparative structural and chemical studies of ferritin cores with gradual removal of their iron contents. J. Am. Chem. Soc. *130*, 8062–8068.
20. Quintana, C., Cowley, J.M., and Marhic, C. (2004). Electron nanodiffraction and high-resolution electron microscopy studies of the structure and composition of physiological and pathological ferritin. J. Struct. Biol. *147*, 166–178.
21. Winklhofer, M., and Kirschvink, J.L. (2010). A quantitative assessment of torque-transducer models for magnetoreception. J. R. Soc. Interface *7*(*Suppl 2*), S273–S289.
22. Nishida, K., and Silver, P.A. (2012). Induction of biogenic magnetization and redox control by a component of the target of rapamycin complex 1 signaling pathway. PLoS Biol. *10*, e1001269.
23. Kim, T., Moore, D., and Fussenegger, M. (2012). Genetically programmed superparamagnetic behavior of mammalian cells. J. Biotechnol. *162*, 237–245.